


# A 4×4 metal-semiconductor-metal rectangular deep-ultraviolet detector array of $Ga_2O_3$ photoconductor with high photo response

Zeng Liu(刘增), Yu-Song Zhi(支钰崧), Mao-Lin Zhang(张茂林), Li-Li Yang(杨莉莉), Shan Li(李山), Zu-Yong Yan(晏祖勇), Shao-Hui Zhang(张少辉), Dao-You Guo(郭道友), Pei-Gang Li(李培刚), Yu-Feng Guo(郭宇锋), and Wei-Hua Tang(唐为华)

**Citation:**Chin. Phys. B, 2022, 31 (**8**): 088503. DOI: 10.1088/1674-1056/ac597d
Journal homepage: http://cpb.iphy.ac.cn; http://iopscience.iop.org/cpb

**What follows is a list of articles you may be interested in**

---

## Fast-speed self-powered PEDOT: PSS/$\alpha$-$Ga_2O_3$ nanorod array/FTO photodetector with solar-blind UV/visible dual-band photodetection

Ming-Ming Fan(范明明), Kang-Li Xu(许康丽), Ling Cao(曹铃), and Xiu-Yan Li(李秀燕)
Chin. Phys. B, 2022, 31 (**4**): 048501. DOI: 10.1088/1674-1056/ac3814

## Deep-ultraviolet and visible dual-band photodetectors by integrating Chlorin e6 with $Ga_2O_3$

Yue Zhao(赵越), Jin-Hao Zang(臧金浩), Xun Yang(杨珣), Xue-Xia Chen(陈雪霞), Yan-Cheng Chen(陈彦成), Kai-Yong Li(李凯永), Lin Dong(董林), and Chong-Xin Shan(单崇新)
Chin. Phys. B, 2021, 30 (**7**): 078504. DOI: 10.1088/1674-1056/abf91c

## Microstructure, optical, and photoluminescence properties of $\beta$-$Ga_2O_3$ films prepared by pulsed laser deposition under different oxygen partial pressures

Rui-Rui Cui(崔瑞瑞), Jun Zhang(张俊), Zi-Jiang Luo(罗子江), Xiang Guo(郭祥), Zhao Ding(丁召), and Chao-Yong Deng(邓朝勇)
Chin. Phys. B, 2021, 30 (**2**): 028505. DOI: 10.1088/1674-1056/abc164

## Rectifying characteristics and solar-blind photoresponse in $\beta$-$Ga_2O_3$/ZnO heterojunctions

Xiao-Fei Ma(马晓菲), Yuan-Qi Huang(黄元琪), Yu-Song Zhi(支钰崧), Xia Wang(王霞), Pei-Gang Li(李培刚), Zhen-Ping Wu(吴真平), Wei-Hua Tang(唐为华)
Chin. Phys. B, 2019, 28 (**8**): 088503. DOI: 10.1088/1674-1056/28/8/088503

## Ultraviolet photodetectors based on wide bandgap oxide semiconductor films

Changqi Zhou(周长祺), Qiu Ai(艾秋), Xing Chen(陈星), Xiaohong Gao(高晓红), Kewei Liu(刘可为), Dezhen Shen(申德振)
Chin. Phys. B, 2019, 28 (**4**): 048503. DOI: 10.1088/1674-1056/28/4/048503

---

# A 4×4 metal-semiconductor-metal rectangular deep-ultraviolet detector array of $Ga_2O_3$ photoconductor with high photo response

Zeng Liu(刘增)[1,2,†], Yu-Song Zhi(支钰崧)[3], Mao-Lin Zhang(张茂林)[1,2], Li-Li Yang(杨莉莉)[1,2], Shan Li(李山)[4], Zu-Yong Yan(晏祖勇)[4], Shao-Hui Zhang(张少辉)[5], Dao-You Guo(郭道友)[6], Pei-Gang Li(李培刚)[4], Yu-Feng Guo(郭宇锋)[1,2], and Wei-Hua Tang(唐为华)[1,2,‡]

[1] *College of Integrated Circuit Science and Engineering, Nanjing University of Posts and Telecommunications, Nanjing* 210023, *China*
[2] *National and Local Joint Engineering Laboratory for RF Integration and Micro-Packing Technologies, Nanjing University of Posts and Telecommunications, Nanjing* 210023, *China*
[3] *China Academy of Launch Vehicle Technology, Beijing* 100076, *China*
[4] *School of Science, Beijing University of Posts and Telecommunications, Beijing* 100876, *China*
[5] *Institute of Microscale Optoelectronics, Shenzhen University, Shenzhen* 518060, *China*
[6] *Center for Optoelectronics Materials and Devices, Department of Physics, Zhejiang Sci-Tech University, Hangzhou* 310018, *China*

(Received 28 October 2021; revised manuscript received 28 February 2022; accepted manuscript online 2 March 2022)

A 4×4 beta-phase gallium oxide ($\beta$-$Ga_2O_3$) deep-ultraviolet (DUV) rectangular 10-fingers interdigital metal-semiconductor-metal (MSM) photodetector array of high photo responsivity is introduced. The $Ga_2O_3$ thin film is prepared through the metalorganic chemical vapor deposition technique, then used to construct the photodetector array via photolithography, lift-off, and ion beam sputtering methods. The one photodetector cell shows dark current of 1.94 pA, photo-to-dark current ratio of $6\times10^7$, photo responsivity of 634.15 A·W$^{-1}$, specific detectivity of $5.93\times10^{11}$ cm·Hz$^{1/2}$·W$^{-1}$ (Jones), external quantum efficiency of 310000%, and linear dynamic region of 108.94 dB, indicating high performances for DUV photo detection. Furthermore, the 16-cell photodetector array displays uniform performances with decent deviation of 19.6% for photo responsivity.

**Keywords:** $Ga_2O_3$, array photodetector, MOCVD, deep UV detection

**PACS:** 85.60.Gz, 29.40.Wk, 95.55.Aq **DOI:** 10.1088/1674-1056/ac597d

## 1. Introduction

Wide and ultra-wide bandgap ($E_g$) semiconductor ultraviolet (UV) photodetectors, owing to their preferable natural properties,[1,2] cater for the desired demands of optical communications, short-distance communications, medical imaging, safety monitoring, environmental protection, and life sciences, etc.[3–8] Among the various wide $E_g$ semiconductors, gallium oxide ($Ga_2O_3$) has the $E_g$ of around 4.8 eV,[9,10] exactly translating to the precise deep-ultraviolet (UV) photo detection,[11–15] along with low false alarming rate. As far as it goes, the $Ga_2O_3$-based deep-UV photodetectors are constructed in the forms of metal-semiconductor-metal (MSM) structures,[16–18] p–n junctions,[19–21] organic–inorganic hybrid heterojunctions,[22–24] Schottky photodiodes,[25–29] field-effect phototransistors,[30–33] and nanorod/nanowire array heterojunction,[34] etc. Such devices have shown excellent optoelectronic performances and provided a promised potential for further developing $Ga_2O_3$-based deep-UV photodetectors. While, these photodetectors are mainly focused on the study of the cell device, in spite of great breakthroughs. For actual applications in imagers, the uniformly high-performance photodetector array is seriously desired.[35–37]

In this respect, Peng *et al.*[38] reported the 32×32, 16×16, 8×8, and 4×4 photodetector arrays with sputtering $Ga_2O_3$ films, in which the 4×4 $Ga_2O_3$ photodetector array displayed a photo responsivity ($R$) of 0.89 A·W$^{-1}$ and an external quantum efficiency (EQE) of 444% at 250 nm UV light irradiation, along with a deviation of 12.1% for $R$. Pratiyush *et al.*[39] displayed a floze-zone grown $Ga_2O_3$ 1×8 photodetector array of 4 A·W$^{-1}$ at 40 V, while it had a large deviation of 62% for dark current ($I_{dark}$). In addition, Zhi *et al.*[40] published a work that a $Ga_2O_3$ 16×4 linear array has shown a high $R$ of 139.56 A·W$^{-1}$ with a deviation of 10%. What's more, Chen *et al.*[41] and Qin *et al.*[42] inhabited the deep-UV imaging application by right of $Ga_2O_3$ photodetector array. The further development is urgently desired for high $R$ and decent deviations. Therefore, a high-performance photodetector array is fabricated and discussed in this paper.

## 2. Experimental details

In this work, we use the metalorganic chemical vapor deposition (MOCVD) to deposit the $Ga_2O_3$ thin film, and then construct the photodetector array through photolithography, lift-off, and ion beam sputtering techniques. The $Ga_2O_3$ thin film are characterized by x-ray diffraction (XRD) and atomic force microscope (AFM). The electrical and optoelec-

†Corresponding author. E-mail: zengliu@njupt.edu.cn
‡Corresponding author. E-mail: whtang@njupt.edu.cn

© 2022 Chinese Physical Society and IOP Publishing Ltd 

trical properties including current–voltage ($I$–$V$) and time-dependent current ($I$–$t$) are measured by a Keithley 4200 semiconductor analysis meter in air at the room temperature. The UV light source is a UV lamp that could emit 254 nm and 365 nm UV light, and the light intensity could be tuned by changing the distance between the photodetector and lamp.

Concretely, the $Ga_2O_3$ thin film was grew on the sapphire substrate by using MOCVD at temperature of 735 °C and chamber pressure of 25 Torr with the [O/Ga] molar ratio of about 1650.[16] Triethylgallium (TEGa) and oxygen are used as the Ga and O sources, and TEGa is kept at temperature of 35 °C and chamber pressure of 760 Torr. Further detailed growth could be seen in Ref. [43]. XRD and AFM are used to characterize the crystal quality of the prepared film, such as the diffraction peaks and root mean square (RMS) roughness.

By photolithography, lift-off, and ion beam sputtering, a $Ga_2O_3$ photodetector array is fabricated as shown in Fig. 1. The symmetrical Ti/Au interdigital metal electrodes are patterned on the surface of the $Ga_2O_3$ thin film. The fabricated photodetector array is annealed in $N_2$ at 200 °C for 60 s, for achieving good Ohmic contacts, in which the electrical and optoelectrical properties is like a photo sensitive conductor. Every photodetector cell is 10 fingers metal-semiconductor-metal (MSM) structure. As shown in Fig. 1, the device scale is 5 μm wide, 190 μm long, and 5 μm spacing distance. As calculated, the effective illuminated area ($S$) of one photodetector cell is 18450 μm$^2$. At last, the current–voltage ($I$–$V$) and time-dependent current ($I$–$t$) performances are measured by employing the Keithley 4200, in order to exam the optoelectrical performances of the prepared photodetector array.

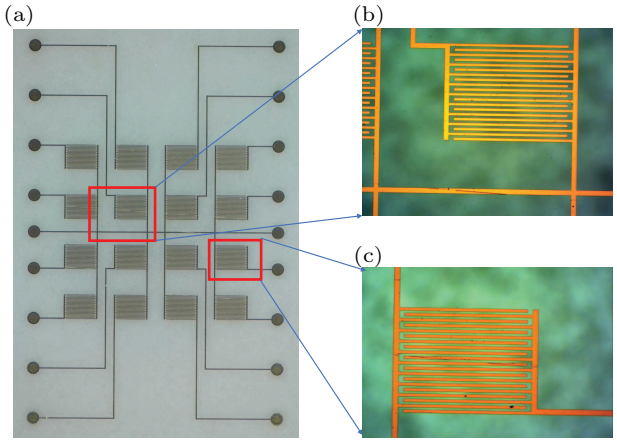



**Fig. 1.** (a) The schematic diagram of the photodetector array, (b) and (c) the images of the enlarged portion of the photodetector array by optical microscope.

## 3. Results and discussion

As shown in Fig. 2(a), the XRD pattern of the MOCVD-grown $Ga_2O_3$ thin film is provided, indicating the ($\bar{2}01$), ($\bar{4}02$), and ($\bar{6}03$) diffraction peaks for $\beta$-$Ga_2O_3$ existence. In addition, the other peaks in the XRD pattern are from the sapphire we used for $Ga_2O_3$ deposition. In Fig. 2(b), the AFM image of the MOCVD-grown ($\bar{2}01$)-oriented $\beta$-$Ga_2O_3$ thin film is shown, suggesting RMS roughness of 6.21 nm, and the AFM scanning area is 10×10 μm$^2$.

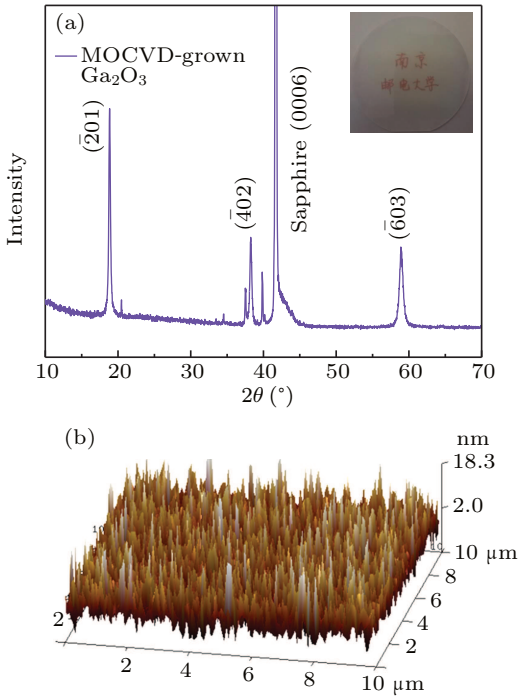



**Fig. 2.** (a) The XRD pattern, and (b) AFM image of the MOCVD-grown $Ga_2O_3$ thin film.

With the aforementioned $Ga_2O_3$ thin film characterized in Fig. 2, the photodetector array is fabricated. The energy-band diagram of one photodetector cell is shown in Fig. 3. Corresponding to the electron affinity of $Ga_2O_3$ [$\chi(Ga_2O_3)\sim$ 4.0 eV] and work function of Ti [$\Phi$(Ti)$\sim$ 4.33 eV], the interfacial barrier at Ti–$Ga_2O_3$ interface ($\Delta\varphi_{Ti-Ga_2O_3}$) is about 0.33 eV. Such a small barrier could guarantee the nearly-Ohmic contact in this device.

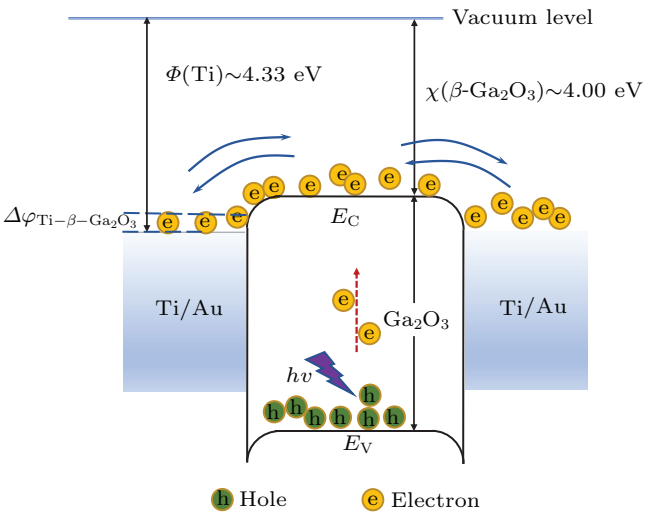



**Fig. 3.** The energy-band diagram of the photodetector cell.

Correspondingly, in Fig. 4(a), for one photodetector cell, the *I*–*V* curves in the dark and under illuminations are expressed, all suggesting sub-Ohmic contacts, on account of the small metal–semiconductor interfacial barrier of Ti–$Ga_2O_3$ according to the Schottky–Mott rule.[44–46] The dark current ($I_{dark}$) is about $1.94\times10^{-12}$ A at bias of 10 V, and the photocurrent ($I_{photo}$) is $6.43\times10^{-5}$ A, $7.59\times10^{-5}$ A, $8.23\times10^{-5}$ A, $1.02\times10^{-4}$ A, $1.17\times10^{-4}$ A, $1.54\times10^{-4}$ A, and $1.74\times10^{-4}$ A under illuminations with light intensity of 400 μW·cm$^{-2}$, 500 μW·cm$^{-2}$, 600 μW·cm$^{-2}$, 800 μW·cm$^{-2}$, 1000 μW·cm$^{-2}$, 1500 μW·cm$^{-2}$, and 2000 μW·cm$^{-2}$, respectively. Correspondingly, the photo-to-dark current ratio (PDCR) is $3.31\times10^7$, $3.91\times10^7$, $4.24\times10^7$, $5.25\times10^7$, $6.0\times10^7$, $7.94\times10^7$, and $8.97\times10^7$, indicating high photo response to 254 nm UV light irradiation. For a photodetector, the *R*, specific detectivity ($D^*$), EQE, and linear dynamic region (LDR) are always used to characterize the photodetector performances. They are expressed as follows:[47–49]

$$R = (I_{photo} - I_{dark})/PS, \tag{1}$$

$$D^* = R/\sqrt{2eI_{dark}/S}, \tag{2}$$

$$\mathrm{EQE} = hcR/e\lambda, \tag{3}$$

$$\mathrm{LDR} = 20\log(I_{photo}/I_{dark}), \tag{4}$$

with *P* as the light intensity, *S* as the effective irradiated area of the photodetector, *e* as the electron charge, *h* as the Planck's constant, *c* as the light speed, and λ as the wavelength (254 nm).

At bias of 10 V and illuminated intensity of 1000 μW·cm$^{-2}$, the *R* is calculated to be 634.15 A·W$^{-1}$, suggesting high photo response of the fabricated photodetector, and lots of electron-hole pairs are photoexcited owing to the highly reaction between the incident photons and the $Ga_2O_3$ matter.[50,51] The $D^*$ is $5.93\times10^{11}$ cm·Hz$^{1/2}$·W$^{-1}$ (Jones), leading to a decent signal/noise performance, where the $I_{dark}$ is considered as the main noise.[48] The EQE is as high as 310000%, and the photodetector cell is well-coupled to the incident 254 nm deep-UV light. In addition, the LDR is 108.94 dB. Without using the constraint of carriers in heterojunctions and Schottky junctions,[22,24,26–28] the MSM photodetector here is superior to the most similar devices.[11,12] On account of two issues: 1) the uniformity of semiconductor and 2) the potential difference caused by electrodes, the charge density and the band diagram are associated with a negatively charged semiconductor surface both in the dark and under illuminations. The presence of a high density of surface bound states for electrons (majority carrier in $Ga_2O_3$) is lying inside the bandgap, and is closing to Fermi level (i.e., the Fermi pinning effect). Therefore, the time evolution of the surface space charge region could be assumed as Schottky diode, as though under open-circuit conditions.[50] The gain (*G*), defined as the increase of collected carriers per absorbed photon, for this photoconductor is mainly from the so-called metal–semiconductor diode, as shown in Fig. 3. The photoconductive *G* can be expressed as

$$G = \frac{\Delta I/q}{P/h\nu}, \tag{5}$$

where Δ*I* is the measured current difference between the conditions of both in the dark and under illuminations, and *hν* is the incident photon energy. So, the *G* can be obtained as 41.01 dB.

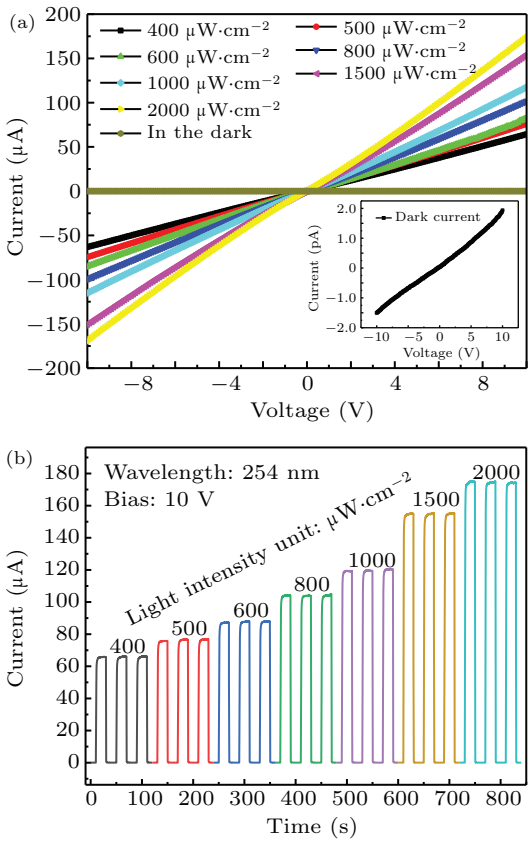



**Fig. 4.** For the photodetector cell. (a) The current–voltage curves under illuminations with different light intensities from 400 μW·cm$^{-2}$ to 2000 μW·cm$^{-2}$ at bias from −10 V to 10 V. (b) The time-dependent current under illuminations with different light intensities from 400 μW·cm$^{-2}$ to 2000 μW·cm$^{-2}$ at bias of 10 V.

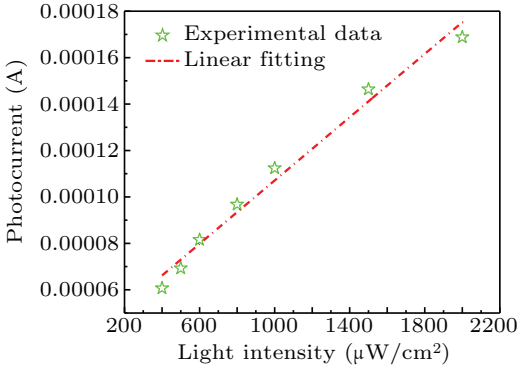



**Fig. 5.** The light intensity-dependent photocurrent of the photodetector cell.

In Fig. 4(b), the *I*–*t* performances of the photodetector cell under illuminations with different light intensities are shown. Higher light intensity contributes to higher $I_{photo}$. Under various light intensity irradiations, the photodetector cell

displays stable and repeatable cycling opto-switching behaviors. As shown in Fig. 5, the $I_{photo}$ displays good linear relationship with the light intensity, indicating that the photodetector may well operate in a linear dynamic region.

Figure 6 displays the $I_{photo}$ and $R$ of the 16 photodetector cells. The deviation of $R$ is estimated to be 19.6% on account of a relationship of $[(R_{max} - R_{ave})/R_{ave}]$,[39] with $R_{max}$ as the maximum $R$, and $R_{ave}$ as the average $R$ for the 16 photodetector cells. It is worthy to be noted that the deviation of $R$ is relatively large. It may well be due to the large RMS of the $Ga_2O_3$ film used for fabricating photodetector array. The photodetectors with films of different thicknesses have different performances,[52] leading to the high $R$ deviation of photodetector array. In addition, the difference of electrode line configuration in all the cells could be another cause for having large deviation. What's more, the $I_{photo}$ and $R$ seem a regular evolution, and we found that the photodetector cells around the photodetector array have higher $I_{photo}$ and $R$, while the photodetector cells in the center area have relatively low $I_{photo}$ and $R$. The photodetector cells in the center area always have long pathway for carrier transports, in which a relatively high resistance leads to a low output $I_{photo}$, thus a low $R$. To some degree, it also decreases the uniform performance of the photodetector array. In all, beyond the study on the cell photodetector, photodetector array is urgently desired for high performances and better uniformity.

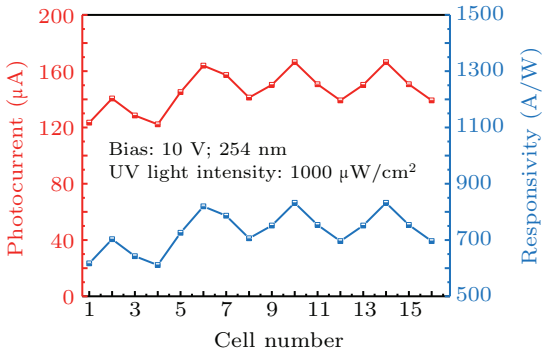



**Fig. 6.** Photocurrents and photo responsivities of the 16 $Ga_2O_3$ deep-UV photodetectors at 10 V bias and under illumination with intensity of 1000 μW/cm$^2$.

## 4. Conclusion

In summary, a 4×4 rectangular photodetector array is introduced based on MOCVD-grown $\beta$-$Ga_2O_3$ thin film. The photodetector cell displays $R$ of 634.15 A·W$^{-1}$, $D^*$ of $5.93\times10^{11}$ Jones, EQE of 310000%, and LDR of 108.94 dB at bias of 10 V and under illumination with light intensity of 1000 μW·cm$^{-2}$, indicating high optoelectronic performances of the fabricated device. And the photoconductive $G$ is 41.01 dB. For the photodetector array with 16 cells, the deviation of $R$ is 19.6%. The good performances of the photodetector described here is owing to the high-quality $\beta$-$Ga_2O_3$ thin film and the successful construction of the array. This work may well provide a promised route for developing the deep-UV photodetection by using $Ga_2O_3$.

## Acknowledgements

Project supported by the National Natural Science Foundation of China (Grant No. 61774019) and Natural Science Research Start-up Foundation of Recruiting Talents of Nanjing University of Posts and Telecommunications (Grant Nos. XK1060921115 and XK1060921002).

## References

[1] Monroy E, Omnes F and Calle D 2003 *Semicond. Sci. Technol.* **18** R33
[2] Xie C, Lu X T, Tong X W, Zhang Z X, Liang F X, Liang L, Luo L B and Wu Y C 2019 *Adv. Funct. Mater.* **29** 1806006
[3] Mueller T, Xia F and Avouris P 2010 *Nat. Photon.* **4** 297
[4] Zheng W, Zhang Z, Lin R, Xu K, He J and Huang F 2016 *Adv. Electron. Mater.* **2** 1600291
[5] Hu Q, Zheng W, Lin R, Xu Y and Huang F 2019 *Carbon* **147** 427
[6] Chen H, Liu K, Hu L, Al-Ghamdi A A and Fang X 2015 *Mater. Today* **18** 493
[7] Shen Y, Yu D, Wang X, Huo C, Wu Y, Zhu Z and Zeng H 2018 *Nanotechnology* **29** 085201
[8] Li F, Ma C, Wang H, Hu W, Yu W, Sheikh A D and Wu T 2015 *Nat. Commun.* **6** 8238
[9] Liu Z, Li P G, Zhi Y S, Wang X L, Chu X L and Tang W H 2019 *Chin. Phys. B* **28** 017105
[10] Higashiwaki M, Sasaki K, Kuramata A, Masui T and Yamakoshi S 2012 *Appl. Phys. Lett.* **100** 013504
[11] Chen X, Ren F, Gu S and Ye J 2019 *Photon. Res.* **7** 381
[12] Xu J, Zheng W and Huang F 2019 *J. Mater. Chem. C* **7** 8753
[13] Kaur D and Kumar M 2021 *Adv. Opt. Mater.* **9** 2002160
[14] Guo D, Guo Q, Chen Z, Wu Z, Li P and Tang W 2019 *Mater. Today Phys.* **11** 100157
[15] Hong L, Hu Z, Zhang H, Xiong Y, Fan S, Kong C, Li W, Ye L and Li H 2021 *J. Mater. Chem. C* **9** 10354
[16] Liu Z, Zhi Y, Li S, Liu Y, Tang X, Yan Z, Li P, Li X, Guo D, Wu Z and Tang W 2020 *J. Phys. D* **53** 085105
[17] Guo D, Wu Z, Li P, An Y, Liu H, Guo X, Yan H, Wang G, Sun C, Li L and Tang W 2014 *Opt. Mater. Express* **4** 1067
[18] Qian L X, Gu Z, Huang X, Liu H, Lv Y, Feng Z and Zhang W 2021 *ACS Appl. Mater. Interfaces* **13** 40837
[19] Liu Z, Zhang S, Zhi Y, Li S, Yan Z, Chu X, Bian A, Li P and Tang W 2021 *J. Phys. D* **54** 195104
[20] Qu Y, Wu Z, Ai M, Guo D, An Y, Yang H, Li L and Tang W 2016 *J. Alloys Compd.* **680** 247
[21] Yu J, Nie Z, Dong L, Yuan L, Li D, Huang Y, Zhang L, Zhang Y and Jia R 2019 *J. Alloys Compd.* **798** 458
[22] Yan Z, Li S, Liu Z, Zhi Y, Dai J, Sun X, Sun S, Guo D, Wang X, Li P, Wu Z, Li L and Tang W 2020 *J. Mater. Chem. C* **8** 4502
[23] Wang H, Chen H, Li L, Wang Y, Su L, Bian W, Li B and Fang X 2019 *J. Phys. Chem. Lett.* **10** 6850
[24] Li S, Yan Z, Liu Z, Chen J, Zhi Y, Guo D, Li P, Wu Z and Tang W 2020 *J. Mater. Chem. C* **8** 1292
[25] Liu Z, Zhi Y, Zhang S, Li S, Yan Z, Gao A, Zhang S, Guo D, Wang J, Wu Z, Li P and Tang W 2021 *Sci. China Tech. Sci.* **64** 59
[26] Liu Z, Li S, Yan Z, Liu Y, Zhi Y, Wang X, Wu Z, Li P and Tang W 2020 *J. Mater. Chem. C* **8** 5071
[27] Jiang W, Liu Z, Li S, Yan Z, Lu C, Li P, Guo Y and Tang W 2021 *IEEE Sens. J.* **21** 18663
[28] Liu Z, Wang X, Liu Y, Guo D, Li S, Yan Z, Tan C K, Li W, Li P and Tang W 2019 *J. Mater. Chem. C* **7** 13920
[29] Wu D, Zhao Z, Lu W, Rogée L, Zeng L, Lin P, Shi Z, Tian Y, Li X and Tsang Y H 2021 *Nano Res.* **14** 1973
[30] Han Z, Liang H, Huo W, Zhu X, Du X and Mei Z 2020 *Adv. Opt. Mater.* **8** 1901833
[31] Yu S, Zhao X, Ding M, Tan P, Hou X, Zhang Z, Mu W, Jia Z, Tao X, Xu G and Long S 2021 *IEEE Electron. Device Lett.* **42** 383

[32] Qin Y, Long S, He Q, Dong H, Jian G, Zhang Y, Hou X, Tan P, Zhang Z, Lu Y, Shan C, Wang J, Hu W, Lv H, Liu Q and Liu M 2019 *Adv. Electron. Mater.* **5** 1900389

[33] Kim S, Oh S and Kim J 2019 *ACS Photon.* **6** 1026

[34] He T, Zhao Y, Zhang X, Lin W, Fu K, Sun C, Shi F, Ding X, Yu G, Zhang K, Lu S, Zhang X and Zhang B 2018 *Nanophotonics* **7** 1557

[35] McClintock R, Mayes K, Yasan A, Shiell D, Kung P and Razeghi M 2005 *Appl. Phys. Lett.* **86** 011117

[36] Lamarre P, Hairston A, Tobin S P, Wong K K, Sood A K, Reine M B, Pophristic M, Birkham R, Ferguson I T, Singh R, Eddy Jr. C R, Chowdhury U, Wong M M, Dupuis R D, Kozodoy P and Tarsa E J 2001 *Phys. Status Solidi A* **188** 289

[37] Yang B, Heng K, Li T, Collins C J, Wang S, Dupuis R D, Campbell J C, Schurman M J and Ferguson I T 2000 *IEEE J. Quantum Electron.* **36** 1229

[38] Peng Y, Zhang Y, Chen Z, Guo D, Zhang X, Li P, Wu Z and Tang W 2018 *IEEE Photon. Technol. Lett.* **30** 993

[39] Pratiyush A S, Muazzam U U, Kumar S, Vijayakumar P, Ganesamoorthy S, Subramanian N, Muralidharan R and Nath D N 2019 *IEEE Photon. Technol. Lett.* **31** 923

[40] Zhi Y S, Liu Z, Zhang S H, Li S, Yan Z Y, Li P G and Tang W H 2021 *IEEE Trans. Electron. Devices* **68** 3435

[41] Chen Y, Lu Y, Liao M, Tian Y, Liu Q, Gao C, Yang C and Shan C 2019 *Adv. Funct. Mater.* **29** 1906040

[42] Qin Y, Li L H, Yu Z, Wu F, Dong D, Guo W, Zhang Z, Yuan J H, Xue K H, Miao X and Long S 2021 *Adv. Sci.* **8** 2101106

[43] Liu Z, Zhi Y, Li S, Liu Y, Tang X, Yan Z, Li P, Li X, Guo D, Wu Z and Tang W 2020 *J. Phys. D* **53** 085105

[44] Schottky W 1939 *Z. Phys.* **113** 367

[45] Mott N F 1939 *Proc. R. Soc. A* **171** 27

[46] Sze S M and Ng K K 2007 *Physics of Semiconductor Devices* (New York: Wiley)

[47] Fang Y, Armin A, Meredith P and Huang J 2018 *Nat. Photon.* **13** 1

[48] Razeghi M and Rogalski A 1996 *J. Appl. Phys.* **79** 7433

[49] Gong X, Tong M, Xia Y, Cai W, Moon J S, Cao Y, Yu G, Shieh C L, Nilsson B and Heeger A J 2000 *Science* **325** 1665

[50] Garrido J A, Monroy E, Izpura I and Munoz E 1998 *Semicond. Sci. Technol.* **13** 563

[51] Kockum A F, Miranowicz A, Liberato S D, Savasta S and Nori F 2019 *Nat. Rev. Phys.* **1** 19

[52] Wang X, Chen Z, Guo D, Zhang X, Wu Z, Li P and Tang W 2018 *Opt. Mater. Express* **8** 2918